

Supplemental material

Daytime feeding with prolonged fasting times reaps greater geroprotective effects when combined with calorie restriction in adult female mice

The document contains 5 supplemental figures and 5 supplemental tables.

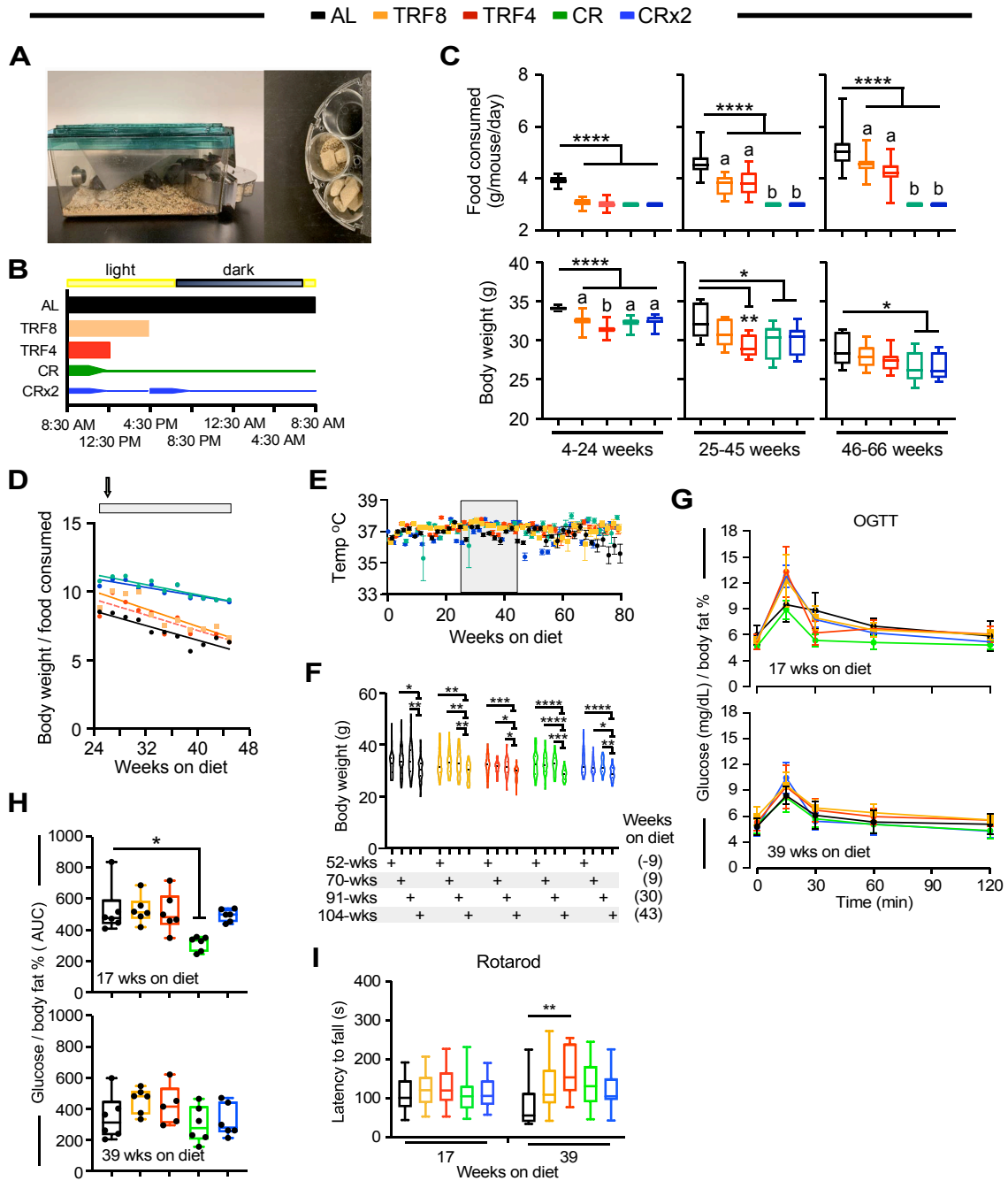


Figure S1. Effect of late onset feeding regime on food consumption, body weight, glucose metabolism, and physical performance in female mice.

(A) Configuration of manual 7-day feeder carousel onto mouse cage.

(B) Graphical representation of the experimental protocol.

(C) Discrete 20-week binning was performed to assess the effect of feeding regime on the amount of food consumed (upper panels) and body weight changes (lower panels): bin 1, 4-24 weeks (left panels); bin 2, 25-45 weeks (middle panels); bin 3, 46-66 weeks (right panels).

(D) Focus on trajectories of body weight (upper panel) and the ratio of 'body weight / amount of food consumed' (bottom panel) for the period between 25-45 weeks after diet switching. Arrow, bleed at 26 weeks for metabolomics analysis. See Data S1 for additional details.

(E) Trajectories of core temperature over the course of 80 weeks under the indicated feeding regimens. Data are expressed as means \pm 95% confidence intervals (CI). Gray box indicates a period of volitional increase in food consumption (25-45 weeks after diet switching) by mice fed AL, TRF8, and TRF4.

(F) Mouse body weight at the onset of body composition assessment by low-field nuclear magnetic resonance imaging. Data distribution is visualized as violin plots with a marker for the median.

(G) Trajectories of blood glucose clearance during an OGTT after normalization by body fat content. Values are represented as means \pm SD. $n = 6$ per group.

(H) Area under the curve (AUC) from the OGTT experiment depicted in panel F.

(I) Latency to fall off the rotarod.

(C,H,I) Values are represented as boxplots depicting minimum, lower quartile (Q1), median (Q2), upper quartile (Q3) and maximum values. Data have been analyzed using one-way ANOVA. *, **, **** $p < 0.05$, 0.01, 0.0001. Different lowercase letters indicate significant differences at $p < 0.05$ (panel C).

Related to Figure 1.

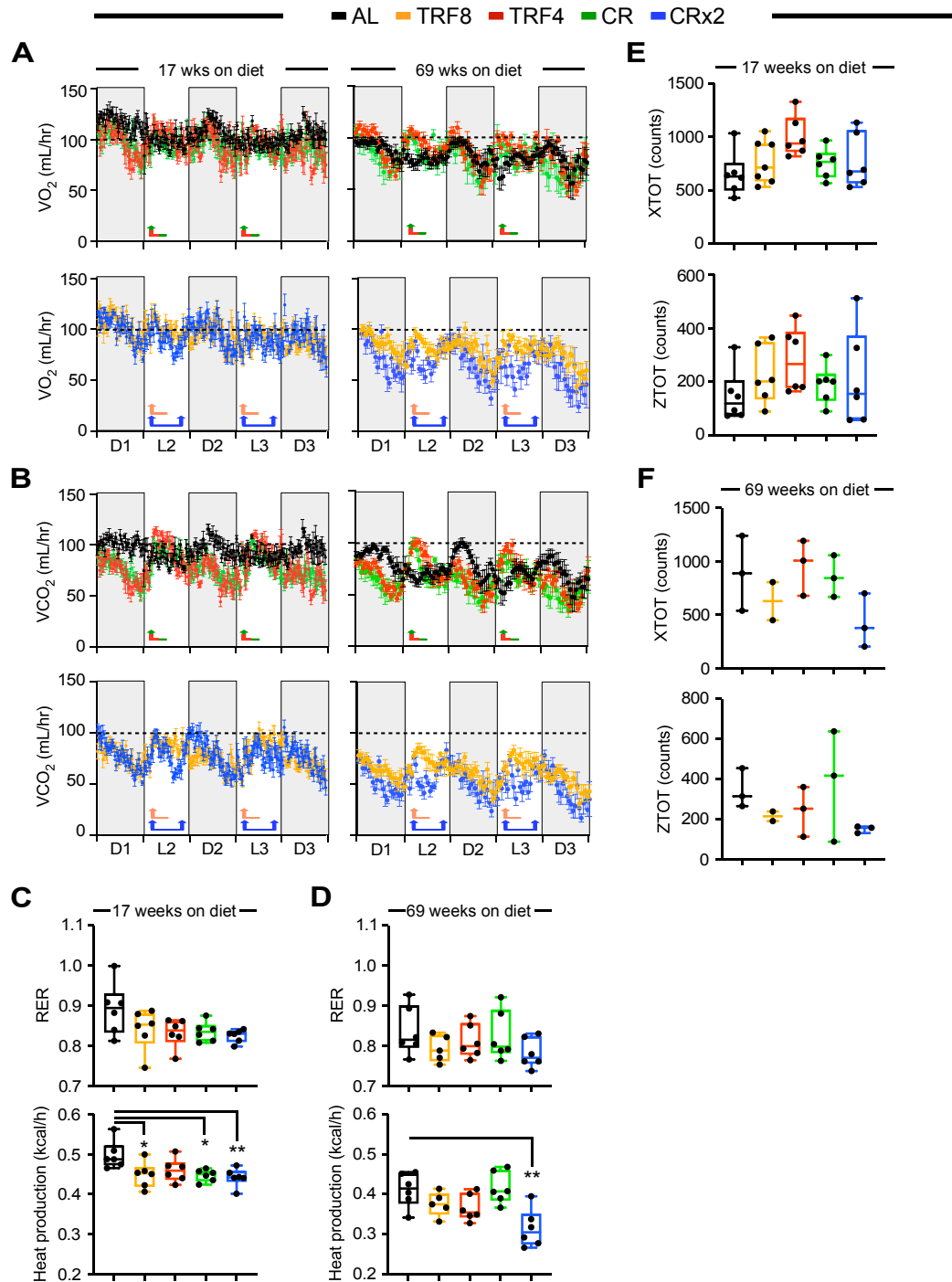


Figure S2. Metabolic adaption to various feeding regimens in female mice.

Mice exposed to the indicated feeding regime for 17 and 69 weeks were placed into metabolic cages for 72 h to measure VO_2 , VCO_2 , respiratory exchange ratio (RER), energy expenditure (EE), and locomotor activity. The values associated with the first 12 h acclimatization phase (L1) were discarded.

(A, B) Averaged hourly trajectories of O₂ consumption (A) and CO₂ production (B) were captured during 3 dark (D) and 2 light (L) cycles. Arrows indicate feeding time (8:30 AM for all groups and 4:30 PM for CRx2 only). Values represent average \pm SD, with n = 6-7 mice per group.

(C, D) The averaged RER (upper panels) and heat production (bottom panels) values were collected over 60 h from metabolic caged mice after a 17-week (C) or 69-week (D) intervention period. Data are represented as box and whisker plots, depicting minimum, lower quartile (Q1), median (Q2), upper quartile (Q3) and maximum values.

(E, F) Locomotor activity in x axis (XTOT, upper panels) and z axis (ZTOT, bottom panels) was measured in metabolic caged mice after a 17-week (E, n=6 mice per group) or 69-week (F, n=2-3 mice per group) intervention period.

One-way ANOVA coupled with Dunnett's post-hoc test was performed.

Related to Figure 2.

Most probable cause of death analysis

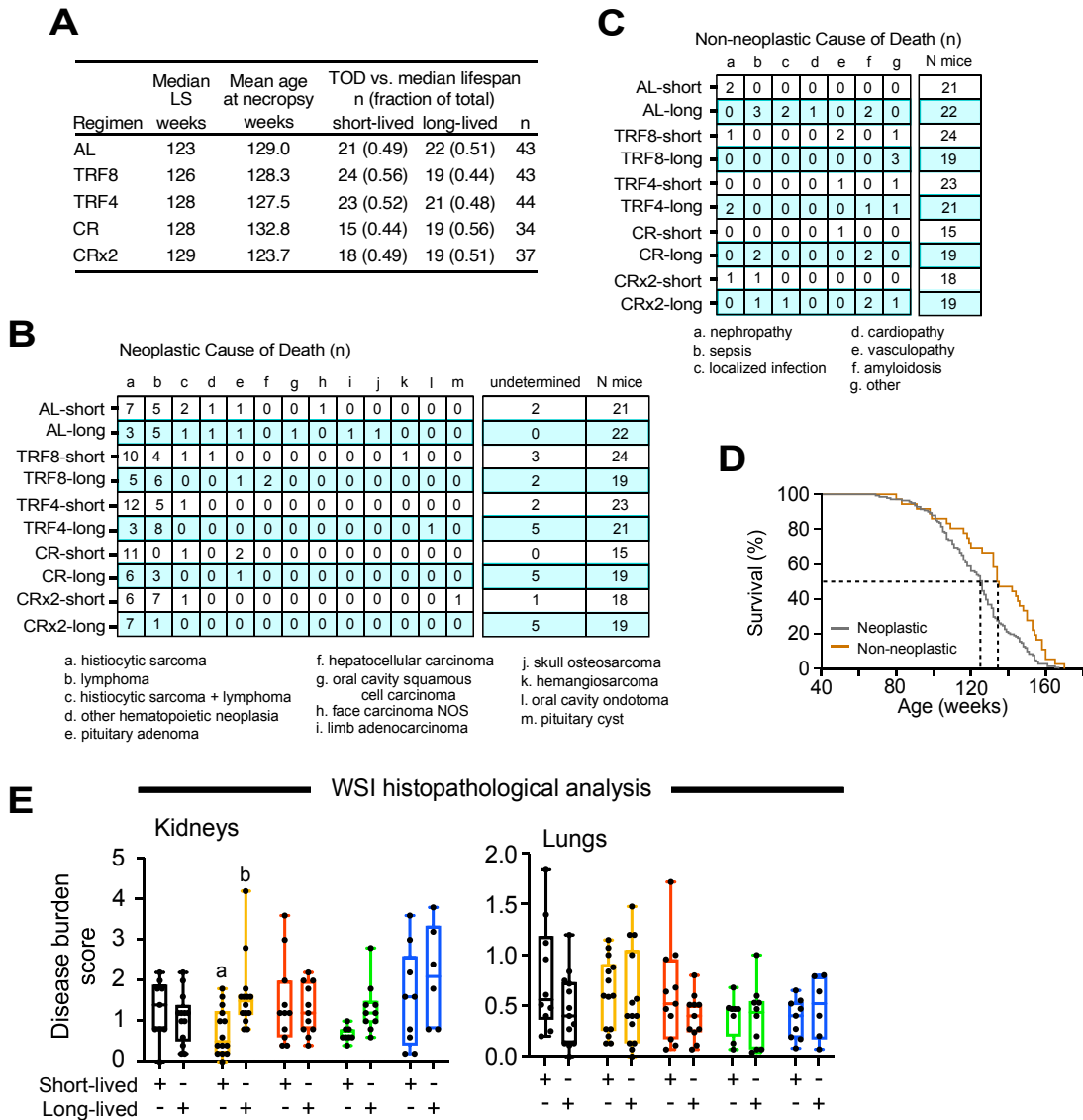


Figure S3. Most probable cause of death assessment at necropsy.

(A) Number, median lifespan (LS), and mean age of female mice at necropsy.

(B, C) Neoplastic (B) and non-neoplastic (C) most probable cause of death. The list of various pathologies and tumor histotypes is represented. (AL, n=43; TRF8, n=43; TRF4, n=44; CR, n=34; CRx2, n=37).

(D) Kaplan-Meier survival curves for female mice from all feeding groups that died with neoplastic (n=141) and non-neoplastic (n= 36) diseases, or from undetermined cause (n = 25). Log-rank (Mantel-Cox) test, $p = 0.0083$.

(E) Whole-slide image (WSI) histopathological analysis of the kidneys and lungs. Two-way ANOVA coupled with Sidak's post-hoc test was performed to assess the effect of feeding regimen, survival [short- vs. long-lived) and their interaction. Data are represented as box and whisker plots, depicting minimum, lower quartile (Q1), median (Q2), upper quartile (Q3) and maximum values. Different letters indicate statistical significance between short- and long-lived mice at $p < 0.05$.

Related to Figure 3B-C.

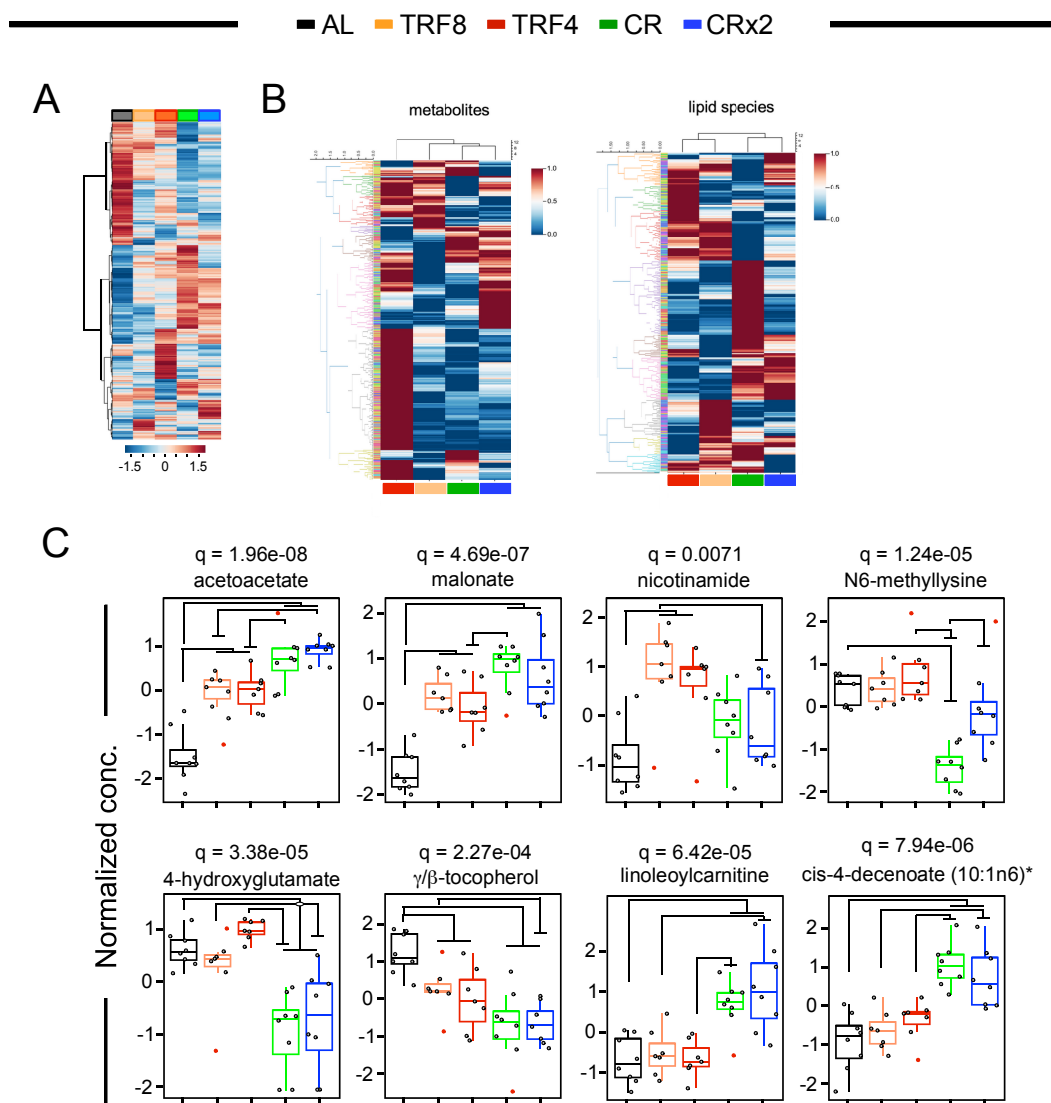


Figure S4. Impact of long-term feeding regimen on serum metabolomics signature in female mice.

The metabolomics data set was analyzed with MetaboAnalyst 5.0.

(A) Group averages of the normalized data using autoscale features. AL, n=8; TRF8, n=7; TRF4, n=7; CR, n=8; CRx2, n=8.

(B) Clustering analysis of metabolites (left panel) and lipid species (right panel) present in the serum of TRF4, TRF8, CR, and CRx2 mice vs. AL-fed controls

(C) Boxplots of select metabolites and lipid species present in the five experimental groups (AL, TRF8, TRF4, CR, CRx2). Data are represented as box and whisker plots, depicting minimum, lower quartile (Q1), median (Q2), upper quartile (Q3) and maximum values. q-values describe false discovery rate (FDR) derived from one-way ANOVA.

Related to Figure 4.

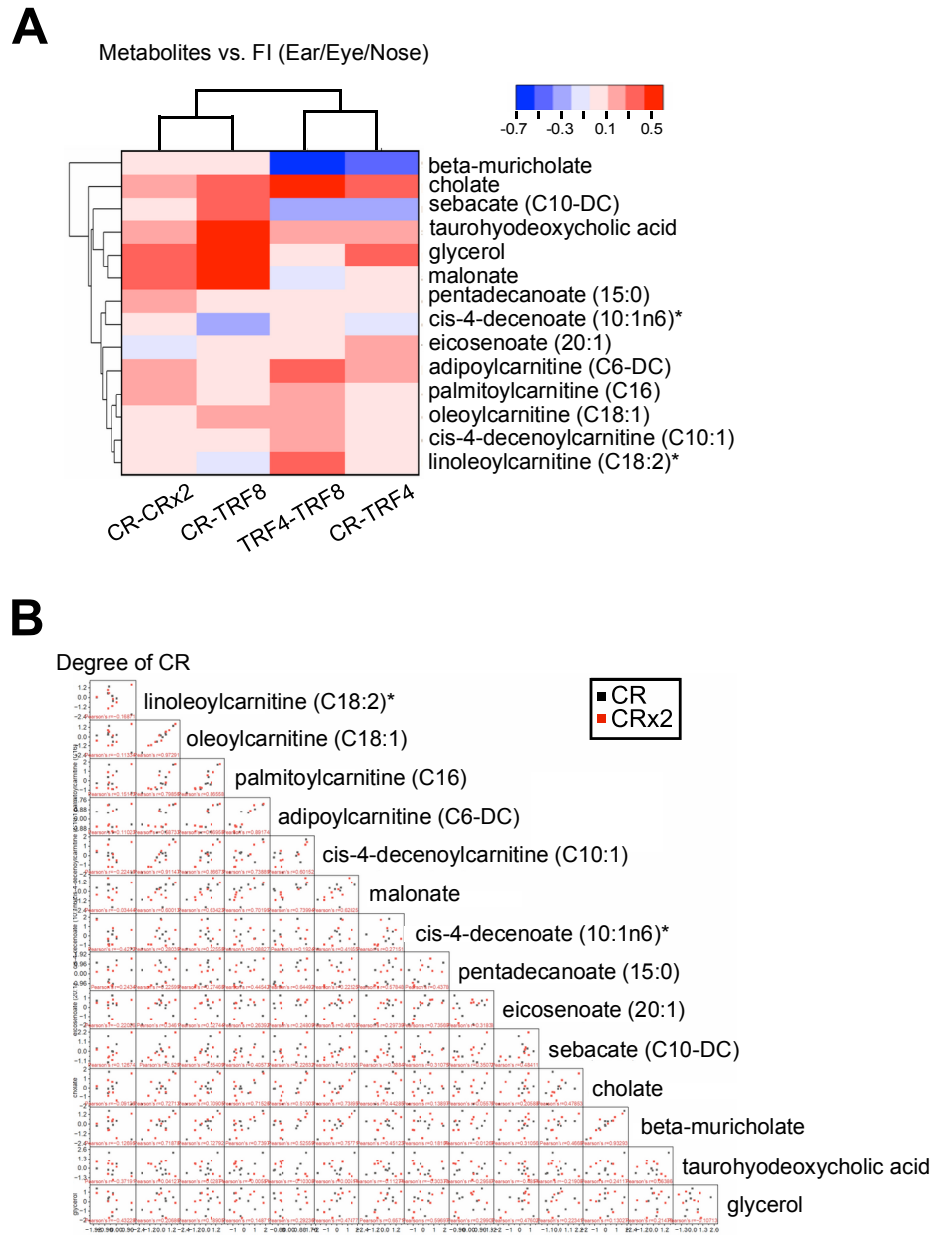


Figure S5. Integrated interpretation of various data sets that includes functional signatures of physiological and metabolic outcomes.

(A) Heatmaps of hierarchically clustered correlation coefficients of metabolites vs. Ear/Eye/Nasal FI component

(B) An example of scatter plot matrix of 14 metabolites vs. degree of CR (1st column) and of each metabolite with respect to each one of the other metabolites; the first column of the matrix shows the Pearson correlation coefficients displayed in the Source Data file for Figure 6A-D.

Related to Figure 6.

Table S1, Related to Figures 1-3 and S3E. Statistical analysis on the effects of feeding regimens on various physiological and energetic outcomes, and disease burden score.

Physiological data (Figures 1 and S1) -two-way ANOVA¹				
Figure panel	Measured outcome	Interaction	Feeding regime	Time on diet
Fig. 1D top	% fat -MRI	F (12, 832) = 0.6460 P = 0.8034	F (4, 832) = 4.266 P = 0.0020, **	F (3, 832) = 44.45 P < 0.0001, ****
Fig. 1D bottom	Lean/fat ratio -MRI	F (12, 822) = 1.707 P = 0.0606	F (4, 822) = 9.535 P < 0.0001, ****	F (3, 822) = 41.24 P < 0.0001, ****
Fig. S1F	Body weight -MRI	F (12, 841) = 0.9003 P = 0.5463	F (4, 841) = 5.358 P = 0.0003, ***	F (3, 841) = 26.41 P < 0.0001, ****
Physiological data (Figures 1 and S1) -one-way ANOVA²				
		F (DFn, DFd)	P value	Kruskal-Wallis
Fig. 1E, baseline	6-h FBG	F (4, 35) = 1.444	0.2402	
Fig. 1E, 26 wks	6-h FBG	F (4, 47) = 40.78	<0.0001, ****	
Fig. 1G, 17 wks	AUC OGTT	F (4, 25) = 3.067	0.0348, *	
Fig. 1G, 39 wks	AUC OGTT	F (4, 25) = 2.753	0.0503	
Fig. 1H, 39 wks	Cagetop (Newtons)		<0.0001, ****	5, 64 = 23.86
Fig. 1I	Frailty index score	F (4, 48) = 7.013	0.0002, ***	
Fig. 1J	Frailty_integumentary	F (4, 48) = 2.581	0.0489, *	
Fig. 1J	Frailty_musculo-skeletal	F (4, 48) = 5.190	0.0015, **	
Fig. 1J	Frailty_ear-eye-nose	F (4, 48) = 3.624	0.0117, *	
Fig. 1J	Frailty_Digestive urogenital	F (4, 48) = 1.189	0.3279	
Fig. 1J	Frailty Breathing	F (4, 48) = 2.772	0.0375, *	
Fig. 1J	Frailty Discomfort	F (4, 48) = 7.075	0.0001, ***	
Fig. S1C, 4-24 wks	Food consumed	F (4, 100) = 200.5	<0.0001, ****	
Fig. S1C, 25-45 wks	Food consumed	F (4, 97) = 85.52	<0.0001, ****	
Fig. S1C, 46-66 wks	Food consumed	F (4, 100) = 107.3	<0.0001, ****	
Fig. S1C, 4-24 wks	Body weight	F (4, 50) = 19.82	<0.0001, ****	
Fig. S1C, 25-45 wks	Body weight	F (4, 50) = 4.752	0.0025, **	
Fig. S1C, 46-66 wks	Body weight	F (4, 50) = 4.235	0.0050, **	
Fig. S1H, 17wks	AUC OGTT/fat %		0.0081, **	5, 30 = 13.75
Fig. S1H, 39 wks	AUC OGTT/fat %	F (4, 24) = 1.832	0.1556	
Fig. S1I, 17 wks	Rotarod (s)	F (4, 111) = 0.7381	0.5680	
Fig. S1I, 39 wks	Rotarod (s)	F (4, 63) = 3.499	0.0121, *	
Metabolic cage data (Figures 2 and S2) -One-way ANOVA²				
Figure panel	Measured outcome	F (DFn, DFd)	P value	
Fig. 2A left, 17 wks	ΔBW (g)	F (4, 25) = 1.806	0.1592	
Fig. 2A right, 69 wks	ΔBW (g)	F (4, 24) = 6.226	0.0014, **	
Fig. 2B left, 17 wks	Food consumed	F (4, 25) = 9.264	<0.0001, ****	
Fig. 2B right, 69 wks	Food consumed	F (4, 24) = 15.58	<0.0001, ****	
Fig. 2C left, 17 wks	Food efficiency	F (4, 25) = 2.281	0.0889	
Fig. 2C right, 69 wks	Food efficiency	F (4, 24) = 3.219	0.0300, *	
Fig. S2C top, 17 wks	RER	F (4, 25) = 2.357	0.0810	
Fig. S2C bot, 17 wks	Heat production	F (4, 25) = 3.963	0.0126, *	
Fig. S2D top, 69 wks	RER	F (4, 24) = 1.214	0.3307	
Fig. S2D bot, 69 wks	Heat production	F (4, 24) = 6.457	0.0011, **	
Fig. 2E top, 17 wks	X-TOT	F (4, 25) = 2.482	0.0686	

Fig. 2E bot, 17 wks	Z-TOT	F (4, 25) = 1.012	0.4202	
WSI -histopathological analysis (Figures 3 and S3E) -two-way ANOVA¹				
Figure panel	Measured outcome	Interaction	Feeding regime	Short vs. long-lived
Fig. 3B - combined	Disease burden score	p=0.0030, **	p=0.0443, *	p=0.0169, *
Fig. 3C – heart		p=0.0668	p=0.0481, *	p=0.0120, *
Fig. 3C – liver		p=0.0006, ***	p=0.1743	p=0.5664
Fig. S3E- kidneys		p=0.0780	p=0.0496, *	p=0.0315, *
Fig. S3E - lungs		p=0.3977	p=0.2575	p=0.2082

¹The results were analyzed by two-way ANOVA with Sidak's post-hoc test.

²The results were analyzed by one-way ANOVA with Dunnett's post-hoc test

Table S2, Related to Figure 3A. Lifespan descriptive statistics and pairwise survival comparisons using Cox Proportional Hazard Regressions.

	Mice (n)	Lifespan (weeks)						
		Min.	P25%	Median	Mean	P75%	P90%	Max.
Overall								
Cohort*	201	69	110	127	125	143	152	170
Subgroup								
AL	43	71	107	123	123	143	149	155
CR	35	80	110	128	129	150	161	170
CRX2	37	69	115	129	127	150	155	167
TRF4	44	73	108	128	125	144	153	160
TRF8	42	83	118	126	125	135	141	154
Group	AL	CR		CRX2		TRF8		
CR	HR=0.56 (0.35-0.90), pval = 0.026*							
CRX2	HR=0.70 (0.45-1.10), pval = 0.080	HR=1.26 (0.79-2.02), pval = 0.361						
TRF8	HR=0.88 (0.58-1.34), pval = 0.528	HR=1.61 (1.02-2.55), pval = 0.069		HR=1.27 (0.82-1.98), pval = 0.312				
TRF4	HR=1.06 (0.70-1.63), pval = 0.612	HR=1.95 (1.22-3.14), pval = 0.016*		HR=1.54 (0.98-2.43), pval = 0.073		HR=1.21 (0.79-1.86), pval = 0.296		

* Only mice that died of natural causes. Abbreviations: P25%, P75%, and P90%, percentile 25, 75, and 90%, respectively; AL, ad libitum; CR, caloric restriction; TRF, time-restricted feeding. HR and pval values were derived from Cox regressions and Log-Rank test, respectively. n= 244 mice (dead: 201; censored: 43).

Table S3, Related to Figure 3B-3D. Modification of the grading system performed according to the guidelines of the geropathology grading system for aging mouse studies set by the Geropathology Research Network*

Amyloid grading	Tumor grading
0: absent	0: absent
1: amyloid deposits in < 25% of the organ	1: benign tumor
2: amyloid deposits in 26-50% of the organ	2: malignant tumor in < 30% of the organ
3: amyloid deposits in 51-75% of the organ	3: malignant tumor in 31-75% of the organ
4: amyloid deposits in > 75% of the organ	2: malignant tumor in >75% of the organ
Disease burden score calculation in following tissues	
Heart	(Amyloid score + fibrosis score + all other lesions sum) / 3
Lung	(Alveolar histiocytosis score + eosinophilic crystalline pneumonia score + inflammation changes average + all other lesions sum) / 5
Kidney	(Glomerular changes sum + tubular changes sum + interstitial changes sum + vascular changes sum + all other lesions sum) / 5
Liver	(Cellular changes sum + inflammation changes sum + vascular changes sum + tumor sum) / 4

* From Snyder et al., 2019.

Table S4. Raw data of the top 25 metabolites responsible for group effects. Related to Figure 4B.

sample name	AL		TRF8		TRF4		CR		CRx2	
	AVG	SD	AVG	SD	AVG	SD	AVG	SD	AVG	SD
trans-4-hydroxyproline	-0.011	0.092	-0.257	0.052	-0.189	0.151	-0.734	0.168	-0.469	0.192
equol sulfate	-0.131	0.314	-0.646	0.244	-0.283	0.425	-2.006	0.422	-1.386	0.277
equol glucuronide	-0.144	0.335	-1.063	0.181	-0.369	0.525	-2.397	0.768	-1.282	0.241
2-(4-hydroxyphenyl)propionate	0.058	0.238	-0.511	0.344	-0.277	0.369	-1.837	0.288	-1.496	0.372
gentisate	-0.329	0.274	-1.467	0.409	-0.935	0.371	-1.940	0.297	-1.730	0.429
genistein sulfate*	-0.086	0.670	-3.419	0.831	-2.844	0.564	-4.336	0.464	-3.304	0.495
diazoin sulfate (2)	-0.318	0.731	-3.460	0.608	-2.916	0.717	-4.039	0.488	-3.655	0.476
glycitein sulfate (2)	-0.427	0.668	-2.722	0.517	-1.718	0.343	-3.021	0.000	-2.954	0.190
2,6-dihydroxybenzoic acid	-0.137	0.650	-1.525	0.239	-1.041	0.315	-1.887	0.413	-1.718	0.245
docosahexaenoylcarnitine (C22:6)	1.072	0.230	-0.073	0.192	0.277	0.271	-0.299	0.539	-0.094	0.199
salicylate	0.155	0.510	-1.061	0.255	-0.644	0.323	-1.619	0.144	-1.496	0.149
lysine	0.245	0.070	-0.197	0.201	-0.016	0.160	-0.397	0.130	-0.277	0.054
acetoacetate	-1.339	0.491	-0.190	0.460	-0.061	0.332	0.447	0.494	0.619	0.210
3-hydroxybutyryllysine**	-1.418	1.108	0.819	0.487	0.546	0.399	1.862	0.580	1.568	0.335
4-hydroxybutyrate (GBH)	-0.300	0.733	1.250	0.395	1.139	0.205	1.933	0.269	1.815	0.344
3-hydroxybutyrate (BHBA)	-0.333	0.744	1.236	0.328	1.109	0.250	1.851	0.283	1.764	0.346
palmitoleate (16:1n7)	-0.207	0.132	0.655	0.178	0.537	0.226	1.055	0.158	0.515	0.303
myristate (14:0)	-0.105	0.185	0.619	0.164	0.631	0.140	1.037	0.164	0.508	0.339
laurate (12:0)	-0.073	0.116	0.514	0.178	0.555	0.131	0.979	0.180	0.481	0.294
10-nonadecenoate (19:1n9)	-0.363	0.110	0.067	0.135	-0.060	0.123	0.365	0.112	0.299	0.229
oleate/vaccenate (18:1)	-0.168	0.090	0.192	0.120	0.133	0.163	0.409	0.121	0.217	0.109
linolenate [alpha or gamma; (18:3)]	-0.359	0.087	0.294	0.154	0.105	0.179	0.709	0.137	0.363	0.346
hexadecadienoate (16:2n6)	-0.209	0.189	0.407	0.250	0.178	0.227	0.943	0.212	0.516	0.288
linoleate (18:2n6)	-0.284	0.060	0.105	0.157	-0.098	0.118	0.383	0.129	0.254	0.144
10-heptadecenoate (17:1n7)	-0.256	0.086	0.190	0.162	-0.035	0.219	0.593	0.143	0.327	0.250

Table S5, related to Figure 4 and Fig. S4. List of serum metabolites significantly and uniquely accumulated in the indicated pairwise comparison. Data were obtained from 4-way Venn diagrams.

HMDB	Metabolites	-Log(P)		
		TRF4_AL	TRF8_AL	Shared_AL
HMDB0000695	4-methyl-2-oxopentanoate	3.644		
HMDB0002064	N-acetylputrescine	0.839		
HMDB0002189	(N(1) + N(8))-acetylspermidine	2.416		
HMDB0003681	4-acetamidobutanoate	1.495		
HMDB0004089	N-formylanthranilic acid	1.945		
HMDB0000821	Phenylacetyl glycine	1.262		
HMDB0041724	dihydroferulic acid sulfate	1.361		
HMDB0000012	2'-deoxyuridine	1.483		
HMDB0000930	Cinnamate	1.658		
HMDB0000622	Ethylmalonate		2.940	
HMDB0006275	dopamine 3-O-sulfate		1.858	
HMDB0240459	4-methylcatechol sulfate		1.741	
HMDB0001406	Nicotinamide			3.571
HMDB0000764	3-phenylpropionate (hydrocinnamate)			3.180
	Metabolites	CR_AL	CRx2_AL	Shared_AL
HMDB0000317	2-hydroxy-3-methylvalerate	1.488		
HMDB0011756	N-acetyl leucine	1.493		
HMDB0000378	2-methylbutyrylcarnitine (C5)	2.173		
HMDB0002038	N6-methyllysine	6.070		
HMDB0038670	S-methylmethionine	2.722		
HMDB0003320	indole-3-carboxylate	3.012		
HMDB29737	3-formylindole	2.714		
HMDB0000232	Quinolate		2.573	
HMDB0000273	Thymidine		1.521	
HMDB0000128	Guanidinoacetate		3.023	
HMDB0000729	2-hydroxybutyrate/2-hydroxyisobutyrate			3.433
HMDB0000396	3-hydroxy-2-ethylpropionate			2.448
HMDB0002035	4-hydroxycinnamate			5.519
HMDB0001344	4-hydroxyglutamate			5.329
HMDB0003464	4-guanidinobutanoate			5.194
HMDB0002108	S-methylcysteine			2.612
HMDB0002302	Indolepropionate			2.857
HMDB0000214	Ornithine			2.983
HMDB0006344	phenylacetylglutamine			3.295
HMDB0001870	Benzoate			2.673
HMDB0062551	4-ethylphenylsulfate			2.162
HMDB0029968	ethyl α -glucopyranoside			4.544
HMDB0240658	2,8-quinolinediol sulfate			2.257
	Lipid species	CR_AL	CRx2_AL	Shared
HMDB0061636	3-hydroxydecanoylcarnitine	3.377		
HMDB0000672	hexadecanedioate (C16-DC)	3.250		
HMDB0000872	tetradecanedioate (C14-DC)	5.033		
HMDB0000131	Glycerol	2.658		
HMDB0005320	1-palmitoyl-2-oleoyl-GPE (16:0/18:1)	3.458		
HMDB0000761	lithocholate	2.030		
HMDB0000874	taurohyodeoxycholic acid	1.976		
HMDB00327	1-palmitoyl-GPA (16:0)	3.920		

HMDB0011561	1-myristoylglycerol (14:0)	3.269		
HMDB0000114	glycerophosphoethanolamine	1.563		
HMDB0000946	ursodeoxycholate		3.060	
HMDB0013205	cis-4-decenoylcarnitine (C10:1)			2.538
HMDB0006469	linoleoylcarnitine (C18:2)*			4.412
HMDB0000792	sebacate (C10-DC)			2.984
HMDB0000409	5-hydroxyhexanoate			2.728
HMDB0002231	eicosenoate (20:1)			2.552
HMDB0007856	1-linoleoyl-GPA (18:2)*			2.328
HMDB0004980	cis-4-decenoate (10:1n6)*			4.212
HMDB0000619	Cholate			3.233
HMDB00502	3-dehydrocholate			2.923
HMDB0240600	1-linoleoyl-GPG (18:2)*			2.564
HMDB0240601	1-palmitoyl-GPG (16:0)*			1.959
HMDB10383	2-palmitoleoyl-GPC (16:1)*			2.578
HMDB0011565	1-palmitoleoylglycerol (16:1)*			3.914
HMDB0011534	2-palmitoleoylglycerol (16:1)*			4.680
HMDB0008105	1-oleoyl-2-linoleoyl-GPC (18:1/18:2)*			2.096
HMDB0008038	1-stearoyl-2-oleoyl-GPC (18:0/18:1)			4.674
	metabolites	CR TRF4	CRx2 TRF8	
HMDB0000729	2-hydroxybutyrate/2-hydroxyisobutyrate	2.822		
HMDB0000532	N-acetylglycine	3.057		
HMDB0000317	2-hydroxy-3-methylvalerate	1.999		
HMDB0000396	3-hydroxy-2-ethylpropionate	2.109		
HMDB0000764	3-phenylpropionate (hydrocinnamate)	0.806		
HMDB0000128	guanidinoacetate	0.870		
HMDB0003464	4-guanidinobutanoate	1.207		
HMDB0038670	S-methylmethionine	3.170		
HMDB0003320	indole-3-carboxylate	1.368		
HMDB0240347	N6-carboxymethyllysine	1.350		
HMDB0000840	2-hydroxyhippurate (salicylurate)	0.694		
HMDB0061880	N-acetyl-beta-alanine		2.384	
HMDB0002035	4-hydroxycinnamate		1.847	
HMDB0001406	nicotinamide		1.477	
HMDB0006335	γ-tocopherol/β-tocopherol		1.990	
HMDB0004983	dimethyl sulfone		1.249	
	Lipid species	CR TRF4	CRx2 TRF8	
HMDB0061677	adipoylcarnitine (C6-DC)	1.949		
HMDB0013207	palmitoleoylcarnitine (C16:1)*	1.885		
HMDB0000691	Malonate	1.991		
HMDB0061859	(14 or 15)-methylpalmitate (a17:0 or i17:0)	2.267		
HMDB0002231	eicosenoate (20:1)	1.869		
HMDB0000826	pentadecanoate (15:0)	2.726		
HMDB0005322	1-palmitoyl-2-linoleoyl-GPE (16:0/18:2)	2.122		
HMDB0001161	deoxycarnitine	1.313		
HMDB0000824	propionylcarnitine (C3)	1.669		
HMDB0002013	butyrylcarnitine (C4)	3.487		
HMDB0094649	2-aminoheptanoate	1.367		
HMDB0010384	1-stearoyl-GPC (18:0)	1.613		
HMDB0010395	1-arachidonoyl-GPC (20:4n6)*	1.237		
HMDB0011130	1-stearoyl-GPE (18:0)	1.342		
HMDB0000227	mevalonate	1.603		

HMDB0011577	1-dihomo-linolenylglycerol (20:3)	1.243		
HMDB0008036	1,2-distearoyl-GPC (18:0/18:0)	1.096		
HMDB0000114	glycerophosphoethanolamine	1.431		
HMDB0000222	palmitoylcarnitine (C16)		0.931	
HMDB0005065	oleoylcarnitine (C18:1)		1.471	
HMDB0000321	2-hydroxyadipate		1.143	
HMDB0000792	sebacate (C10-DC)		1.199	
HMDB0007856	1-linoleoyl-GPA (18:2)*		1.213	
HMDB0000355	3-hydroxy-3-methylglutarate		1.373	
HMDB0000415	beta-muricholate		1.996	
HMDB0000619	Cholate		2.277	
HMDB0000733	hyodeoxycholate		1.298	
HMDB0000811	6-beta-hydroxylithocholate		2.097	
HMDB0000946	ursodeoxycholate		3.372	
HMDB00502	3-dehydrocholate		2.701	
HMDB0004949	N-palmitoyl-sphingosine (d18:1/16:0)			1.172
HMDB0240684	ceramide (d18:1/20:0, d16:1/22:0, d20:1/18.0)*			1.570
HMDB0000126	glycerol 3-phosphate			1.198
HMDB10383	2-palmitoleoyl-GPC (16:1)*			2.713
HMDB0008038	1-stearoyl-2-oleoyl-GPC (18:0/18:1)			1.745
HMDB0008147	1-linoleoyl-2-arachidonoyl-GPC (18:2/20:4n6)*			3.959

Typeset: AL, **black**; TRF4, **red**; TRF8, **orange**; CR, **green**; CRx2, **blue**.